Electrical Sensor Array for Polymerase Chain Reaction–Free Messenger RNA Expression Profiling

ARTICLE *in* ANALYTICAL CHEMISTRY · JULY 2010

Impact Factor: 5.64 · DOI: 10.1021/ac1003135 · Source: PubMed

4 AUTHORS, INCLUDING:

Somenath Roy
Central Glass and Ceramics Research Instit…
31 PUBLICATIONS **528** CITATIONS
SEE PROFILE

Zhiqiang Gao
National University of Singapore
142 PUBLICATIONS **4,255** CITATIONS
SEE PROFILE

Anal. Chem. **2010,** *82,* 5958–5964

Electrical Sensor Array for Polymerase Chain Reaction-Free Messenger RNA Expression Profiling

Xiaojun Chen, Somenath Roy, Yanfen Peng, and Zhiqiang Gao*

Institute of Bioengineering and Nanotechnology, 31 Biopolis Way, Singapore 138669

A simple and sensitive electrical sensor array for polymerase chain reaction-free (PCR-free) messenger RNA (mRNA) expression profiling is described in this work. The sensor array, consisting of vertically aligned gold microband electrode/SiO_2/gold microband electrode sandwich structures (nanogap sensors) in orthogonal configurations, was fabricated on a 1 cm $\times$ 1 cm silicon chip. A target mRNA was first hybridized with its specific capture probes (CP) on the bottom side of the nanogap, followed by a second hybridization (annealing) of its poly(A) tail with poly(T) annealing probes (AP) on the top side of the nanogap, holding the hybridized mRNA strands vertically across the nanogap. A subsequent metallization of the hybridized mRNA strands bridged the nanogap and consequently produced a substantial change in conductance, allowing ultrasensitive detection of mRNA without any amplification. Noticeable conductance changes were observed in the presence of as little as 0.10 fM mRNA. A linear relationship between the conductance and mRNA concentration was obtained from 0.50 fM to 1.0 pM with exceptional signal intensity. As little as a 50% difference in mRNA expression was successfully detected. The sensor array also exhibited excellent mismatch discrimination due to its unique vertically aligned nanostructure and the two-step hybridization.

It has become apparent that quantification of gene (messenger RNA, mRNA) expression is a powerful tool for in-depth understanding of the biology underlying complex physiological conditions. Changes in expression of mRNAs can also be the indicators of specific genetic diseases, such as cancer.[1] Conventional techniques for mRNA expression profiling include Northern blot,[2] ribonuclease protection analysis,[3] quantitative polymerase chain reaction (qPCR),[4,5] and microarray.[6−8] The first two techniques are laborious and insensitive, require 10−100 μg of total RNA, and can detect single mRNAs at 10^6−10^7 copy levels.[2,3] Recent attempts to quantify mRNA expression have been focused on the use of PCR and fluorometric detection. For example, mRNA expression profiles can be established on an individual gene basis by using reverse transcription (RT) and qPCR[4,5] and at the level of the whole genome by using microarray coupled with PCR.[6−8] Despite their extensive analytical capabilities, the use of qPCR and microarray for clinical diagnostics is not yet prevalent as the full exploitation of these two PCR-based technologies, however, is still limited by technical challenges, such as the high cost and low throughput in RT-qPCR and cross-hybridization when tens of thousands of capture probes interact with different characteristics of mRNA under identical conditions in microarray.[4−8] Moreover, the efficiency of RT reaction and PCR amplification could introduce bias, as any minute variation introduced in any of the processes, from sample preparation and primer set selection and optimization to PCR and hybridization, can greatly influence the precision and quality of the resulting data,[9−12] restricting the use of microarray in research laboratories.

To alleviate the aforementioned drawbacks of PCR-based techniques, substantial research efforts have been devoted to the development of direct detection techniques for mRNA.[13−23] Microarray allows genotyping of thousands of genes in one run and is most suitable for large-scale association studies.[6−8] However, it is anticipated that, eventually, a small group of genes will be assessed routinely in a molecular diagnostic laboratory. The detection of specific mRNA transcripts will be used to identify subtypes of a disease and to determine the gene expression for early diagnosis and monitoring of treatment progress. There are

* To whom correspondence should be addressed. E-mail: zqgao@ibn.a-star.edu.sg. Phone: +65 6824-7113. Fax: +65 6478-9085.

(1) Morris, S. R.; Carey, L. A. *Curr. Opin. Oncol.* **2007**, *19*, 547–551.
(2) White, B. A.; Bancroft, F. C. *J. Biol. Chem.* **1982**, *257*, 8569–8572.
(3) Zhou, L.; Otulakowski, G.; Lau, C. Y. *Methods Enzymol.* **1997**, *282*, 64–76.
(4) Pahl, A. *Expert Rev. Mol. Diagn.* **2005**, *5*, 43–52.
(5) VanGuilder, H. D.; Vrana, K. E.; Freeman, W. M. *BioTechniques* **2008**, *44*, 619–626.
(6) Noordewier, M. O.; Warren, P. V. *Trends Biotechnol.* **2001**, *19*, 412–415.
(7) Muyal, J. P.; Singh, S. K.; Fehrenbach, H. *Crit. Rev. Biotechnol.* **2008**, *28*, 239–251.
(8) Imbeaud, S.; Auffray, C. *Drug Discovery Today* **2005**, *10*, 1175–1182.
(9) Baugh, L. R.; Hill, A. A.; Brown, E. L.; Hunter, C. P. *Nucleic Acids Res.* **2001**, *29*, e29.
(10) Wang, J.; Hu, L.; Hamilton, S. R.; Coombes, K. R.; Zhang, W. *BioTechniques* **2003**, *34*, 394–400.
(11) Wang, E. *J. Transl. Med.* [Online] **2005**, *3*, 28 (July 25, 2005). http://www.translational-medicine.com/content/3/1/28.
(12) Draghici, S.; Khatri, P.; Eklund, A. C.; Szallasi, Z. *Trends Genet.* **2006**, *22*, 101–109.
(13) Homola, J. *Anal. Bioanal. Chem.* **2003**, *377*, 528–539.
(14) Waggoner, P. S.; Craighead, H. G. *Lab Chip* **2007**, *7*, 1238–1255.
(15) Lucarelli, F.; Tombelli, S.; Minunni, M.; Marrazza, G.; Mascini, M. *Anal. Chim. Acta* **2008**, *609*, 139–159.
(16) Sassolas, A.; Leca-Bouvier, B.; Blum, L. J. *Chem. Rev.* **2008**, *108*, 109–139.
(17) Cole, K.; Truong, V.; Barone, D.; McGall, G. *Nucleic Acids Res.* **2004**, *32*, e86.
(18) Huang, Z.; Alsaidi, M. *Anal. Biochem.* **2003**, *322*, 269–274.
(19) Alsaidi, M.; Elena, L. E.; Huang, Z. *ChemBioChem* **2004**, *5*, 1136–1139.
(20) Anthony, R. M.; Schuitema, A. R. J.; Oskam, L.; Klatser, P. R. *J. Microbiol. Methods* **2005**, *60*, 47–54.
(21) Xie, H.; Yu, Y. H.; Lao, Y. Z.; Gao, Z. Q. *Anal. Chem.* **2004**, *76*, 4023–4029.
(22) Lee, A. C.; Dai, Z. Y.; Chen, B. W.; Wu, H.; Wang, J.; Zhang, A. G.; Zhang, L. R.; Lim, T. M.; Lin, Y. H. *Anal. Chem.* **2008**, *80*, 9402–9410.
(23) Fang, Z. C.; Kelley, S. O. *Anal. Chem.* **2009**, *81*, 612–617.

10.1021/ac1003135
Published on Web 06/25/2010

ever-increasing needs for expression profiling of mRNAs at low to medium density (<1000). In addition, it is critical to accurately estimate the proportional expression of distinct mRNA transcripts since such proportions directly correlate to cell function by modulating protein expression. Unfortunately, direct detection of mRNA with high sensitivity still remains a grand challenge. For example, direct electrochemical detection of nucleobases in mRNA and most of the label-free techniques, such as quartz crystal microbalance, surface plasmon resonance, and cantilevers, are unable to meet the sensitivity (≤femtomolar) required for mRNA expression profiling.[13−16] As compared to the hundreds of PCR-based gene analysis reports, so far, only a few attempts have been made in the past years.[17−23] In most cases, to detect mRNA directly, chemical/biological ligations have to be the first step. Cole et al. developed a T4 RNA ligase procedure to couple biotinylated nucleotides to mRNA directly, thereby avoiding the use of RT-PCR.[17] Huang and co-workers reported a two-enzyme approach, RNase H digestion to remove the 3′-poly(A) tail and subsequent Klenow extension to direct label mRNA with a detectable tag in total RNA.[18,19] A simple nonenzyme approach for direct detection of mRNA, in which a pair of fluorophore-tagged oligonucleotide probes were hybridized to the mRNA of interest captured on a microarray, was proposed by Anthony et al.[20] It was demonstrated that femtomoles of mRNA can be detected in total RNA extracted from a bacterial culture.

To accomplish high sensitivity, the direct chemical/biochemical ligation in conjunction with non-PCR amplification so far has been the best bet. In an early report, Xie et al. proposed a cisplatin-based chemical ligation procedure for mRNA.[21] More recently, branched-DNA (bDNA)[22] and direct electrocatalysis[23] were reported for PCR-free electrochemical detections of mRNAs. The former utilizes the bDNA as detection probes for signal amplification, and the latter engages peptide nucleic acid (PNA) capture probes coupled with electrostatic interaction and electrocatalysis. Being charge neutral, the PNA capture probes produce a clean background. Upon hybridization, a negatively charged surface is formed, originated from the phosphate groups on the mRNA backbones. When the hybridized biosensor is incubated in $Ru(NH_3)_6^{3+}$ solution, the cationic $Ru(NH_3)_6^{3+}$ is concentrated around the hybridized mRNA strands through electrostatic interaction between $Ru(NH_3)_6^{3+}$ and the phosphate backbones. It is shown that the $Ru(NH_3)_6^{3+}$ at the biosensor surface acts as an electrocatalytic reporter for signal amplification. The biosensor is able to detect a target mRNA at 0.10 pM in the presence of a large excess of coexisting noncomplementary RNA sequences.

Nonetheless, the much needed sensitivity and multiplexing capability in mRNA expression profiling remain to be realized. A method sensitive enough to detect specific mRNAs without any ligation and amplification is preferred for gene expression profiling. The use of electrical techniques in principle allows for the development of a simple, rapid, and portable DNA detection platform. Recent advances in nanotechnology have open up new opportunities for electrical detection of mRNA.[24,25] In this report, we showed an adaptation of a two-step hybridization scheme in conjunction with a nanogap-based sensor array to enhance the sensitivity and lower the detection limit. The applicability of the sensor array in PCR-free mRNA expression profiling in total RNA was demonstrated. Different from other electrical sensor arrays previously published,[24,25] a second hybridization anneals mRNA strands across the nanogap. And subsequently utilizing the mRNA strands as templates for the formation of silver nanowires "bridges" the nanogap. Messenger RNA can be conveniently detected with superior sensitivity and signal intensity by simply measuring the conductance change across the nanogap. Thus, the sensor array presented here can serve as the foundation for future development of a quantitative and multiplexing mRNA expression assay.

Table 1. Oligonucleotide Capture Probes Used in the Study

gene (mRNA)	capture probe sequence	T_m (°C)
GAPDH	3′-HS−$(CH_2)_6$−TGTACCGGAGGTTCCCTCATT-5′	58
BRCA1	3′-HS−$(CH_2)_6$−GGACTATGAAAAGACCTACGGAG-5′	58
His4	3′-HS−$(CH_2)_6$−TCCATTGACGTAGCGCCTAA-5′	58
annealing probe	3′-TTTTTTTTTTTTTTTTTT−$(CH_2)_6$−SH-5′	36

EXPERIMENTAL SECTION

Chemicals and Materials. Thiol-terminated DNA capture probes (CP) and poly(T) annealing probes (AP) (Table 1) used in this work were custom-made by Sigma-Genosys (Woodlands, TX) and used as received. Other oligonucleotides were from 1st Base Pte Ltd. (Singapore). All other reagents were purchased from Sigma-Aldrich (St. Louis, MO) and used without further purification. Phosphate-buffered saline (PBS, 10 mM phosphate buffer + 139 mM NaCl + 2.7 mM KCl) was used in probe immobilization. A pH 8.5 10 mM Tris-HCl−1.0 mM EDTA−0.10 M NaCl (TE) buffer solution was used as the first hybridization and a TE buffer containing 50 mM $MgCl_2$ (TEM) was used as the second hybridization and washing buffer. The presence of Mg^{2+} elevates the melting temperature of poly(A)−poly(T) duplexes and enhances the hybridization efficiency of the annealing process. Messenger RNA standards (cDNA) were RT-PCR products of the corresponding mRNAs. Tissues samples were snap-frozen on arrival and stored in liquid nitrogen until use. Total RNA was extracted by using TRIzol reagent (Invitrogen, Carlsbad, CA) according to the manufacturer's recommended protocol. The yield and quality of the total RNA were routinely assessed by gel electrophoresis and UV spectrometric measurements.[21] To minimize the effect of RNase on the stability of RNA, autoclaved and diethyl dicarbonate treated nanopore water was used for all buffer and sample preparations and all surfaces were decontaminated with RNaseZap (Ambion, TX).

Nanogap Sensor Array Fabrication. The sensor array was fabricated on a 1 cm ×1 cm silicon chip with 500 nm coating of SiO_2 by using standard photolithographic techniques similar to our previous report.[26] In brief, a 4 in. silicon wafer coated with 500 nm SiO_2 was first photolithographically patterned with a photoresist to realize the bottom gold electrodes. A 10−20 nm SiO_2 insulating layer was deposited on the entire wafer after

(24) Roy, S.; Gao, Z. Q. *Nano Today* **2009**, *4*, 318–334.
(25) Rosi, N. L.; Mirkin, C. A. *Chem. Rev.* **2005**, *105*, 1547–1562.
(26) Roy, S.; Chen, X. J.; Li, M. H.; Peng, Y. F.; Anariba, F.; Gao, Z. Q. *J. Am. Chem. Soc.* **2009**, *131*, 12211–12217.

realizing the bottom gold electrodes by a plasma-enhanced chemical vapor deposition method using tetraethoxyorthosilicate (TEOS) vapor as a source for silicon and O_2 as precursor gas under well-optimized conditions. Ellipsometric measurements indicated that there was only <0.5 nm variation in the SiO_2 layer thickness with a roughness of <1.0 nm over the entire wafer. Another photolithographic process was then performed to pattern the wafer for the top electrodes followed by a rf magnetron sputtering of Au on a Ti adhesion layer. After lift-off, the wafer was placed in a reactive ion etching (RIE) chamber for a selective and complete removal of the SiO_2 layer from the undesired portion of the bottom electrodes. In this case, the top gold layer stack acted as a well-defined mask for etching the SiO_2 layer and microscopic observations suggested that reasonably sharp edges and smooth gold surfaces were obtained.[26]

Capture Probe Immobilization. The proposed approach of utilizing the nanogap to detect mRNA involves a pair of oligonucleotide capture probes, namely, the CP and AP, for each target mRNA strand. The characteristics of the CPs are unique to their respective target mRNAs to be detected and have similar melting temperatures. And the APs (poly(T)) are complementary to the poly(A) tails of all mRNAs and have exactly the same length. Before probe immobilization, the array chip was first cleaned in Nanostrip[27] solution for 15 min to remove any organic residues or remnant photoresist, thoroughly rinsed with water, and soaked in AP solution for 2 h to introduce AP monolayers on the nanogap structures. The bottom gold bands (electrodes) of the sensor array were activated for CP immobilization by selectively removing the monolayer from their surfaces.[26] Briefly, the electrodes were subjected to electrochemical stripping that would selectively and completely remove the monolayer from their surfaces. A single potential cycling was performed between −1.0 and 1.0 V (vs Ag/AgCl) at a scan rate of 200 mV/s. Then, a 2.0 μL droplet of 1.0 μM CP solution was applied to the electrodes. After 2 h of incubation at room temperature, it was rinsed with copious amount of water and dried in a stream of nitrogen. At this stage, one could expect a monolayer of CP on the activated electrodes only. Subsequent activation−immobilization cycles introduced oligonucleotide probes onto desired electrodes. The array chip was ready after a thorough wash with water.

Hybridization and Detection. The nanogap sensor array was treated with an aliquot of 20 μL of total RNA in TE buffer where target mRNAs were hybridized to the surface-bound CPs on the bottom electrodes at 50 °C. The sensor array then underwent three stringency washes with SSC buffer (80 mM NaCl + 8 mM sodium citrate + 0.1% sodium dodecyl sulfate; 5−7 °C below melting temperature) to remove any nonspecifically adsorbed or partially hybridized mRNA strands. Thereafter, it was soaked in TEM buffer at room temperature. At this stage, the poly(A) tails of the hybridized mRNAs on the bottom electrode further hybridized with the AP on the top electrodes, forming mRNA "bridges" across the nanogaps. Finally, the hybridized mRNA strands were made electrically conducting by a simple mRNA-templated formation of silver nanowires alongside the mRNA strands as follows:[28] The hybridized sensor array was incubated in 0.10 M $AgNO_3$ in ammonia (pH = 10.5) for 10 min. After a brief rinsing, the adsorbed silver ions were reduced by 50 mM hydroquinone in ammonia (pH = 10.5). Conductance measurements were performed with a parameter analyzer. To better visualize the silver nanowires, further silver enhancement was applied to the samples for scanning electron microscopic (SEM) experiments. That is, after the silver ion collection and reduction, a mixture of 1.0 mM $AgNO_3$ and 2.0 mM hydroquinone in pH 3.5 citrate buffer was applied onto the array for a certain period of time. Usually 5−10 min was sufficient to form highly visible silver nanowires under SEM.

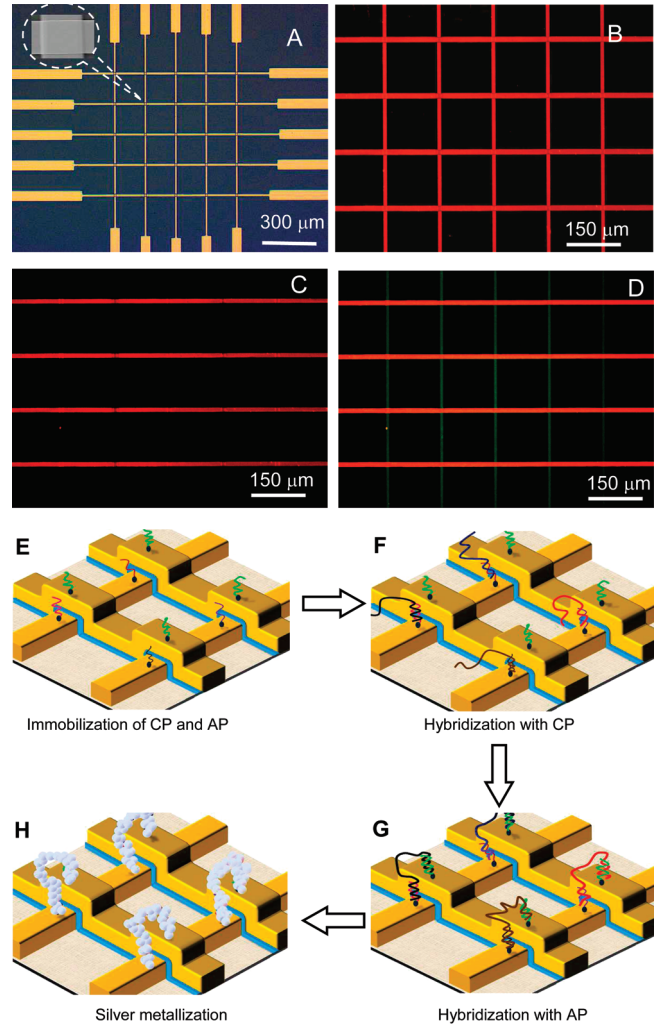

Figure 1. (A) Optical image of a cluster of 5 × 5 pairs of nanogapped microelectrodes fabricated on a 1 cm × 1 cm silicon chip. Inset: an SEM image of the nanogap. Fluorescence images of the 5 × 5 cluster of the sensor array (B) after AP immobilization, (C) after electrochemical stripping, and (D) after CP immobilization on the bottom electrodes. Hybridization with a mixture of 1.0 μM FAM (green dye)-labeled oligonucleotides with their base sequences complementary to CPs, and Cy3 (red dye)-labeled oligonucleotides with their base sequence complementary to AP, was performed after each treatment. (E−H) Schematic illustration of the two-step hybridization and electrical sensing mechanism.

RESULTS AND DISCUSSION

Sensor Array Fabrication. Illustrations of the nanogap device along with the sensing procedure are depicted in Figure 1. An optical image of a representative cluster, consisting of 25 individual

(27) Nanostrip solution is a mixture of H_2SO_4, H_2SO_5, H_2O_2, and water, available commercially from Cyantek Corporation.
(28) Braun, E.; Eichen, Y.; Sivan, U. *Nature* **1998**, *391*, 775–778.

nanogap sensors, is shown in Figure 1A. Between 20 and 80 clusters can be fabricated on the 1 cm ×1 cm chip, mainly limited by the size of connection pads (pitch size of our jig) for electrical measurements. Higher density is possible with a better precision tool for the electrical measurements. The clusters are sufficiently spaced from each other so that each cluster can be independently manipulated by ≤2 μL droplets. Vital to the feasibility of this approach is to have an excellent insulating SiO_2 layer, or a nominal leakage current of the blank sensor array, which should at least be an order of magnitude lower than the lowest signal generated after the mRNA bridging. In general, the leakage current is primarily due to tunneling of charge carriers through the SiO_2 layer in the relatively large common area of the electrodes (10 μm × 12 μm). It is known that the morphology, compactness, and homogeneity of the SiO_2 layer play a crucial role in determining the leakage current. Several optimization experiments were therefore performed to obtain a very smooth, compact, and homogeneous SiO_2 layer. For example, a 45 s deposition time with O_2 and TEOS vapor flow rates of 2000 sccm and 0.5 L/min, respectively, at a chamber pressure of 850 mTorr, gave us a 20 ± 0.4 nm SiO_2 layer with surface roughness of <0.5 nm and a leakage current of <1.0 pA. Since the roughness of the bottom gold electrode dictates the performance of the array, great care was taken in the deposition of the bottom gold electrodes. A series of optimization experiments were carried out when fabricating the nanogap, and detailed atomic force microscopic characterizations of the gold surface were performed. Under selected conditions, the roughness of the gold layer was well within 2 nm. Well-defined sidewalls (nanogaps) of the insulating layer and the top gold electrode, necessary for mRNA bridging, were produced by RIE using the top gold layer as a natural mask.

Contrary to micro/nanogap structures in planar configurations, where fabricating reproducible nanogaps remains a technical challenge, utilizing the SiO_2 layer to define the nanogap width and the side walls as the nanogap device in the vertically aligned gold/SiO_2/gold sandwich structure, good nanogap structures can easily be fabricated through adjusting experimental variables in the SiO_2 deposition process. With the use of this process we have fabricated nanogap sensor arrays of different gap sizes that varied from 10 to 100 nm with precise control of gap size (< ±1.0 nm) with high device uniformity and unlimited scalability. In principle, detections of target mRNA strands ≥50 bases can be performed at 5 nm nanogap sensor arrays, which covers all known genes in eukaryotic organisms.[29] To realize the architecture of the nanogap sensing, the CP and AP pairs have to be immobilized on the two corresponding gold electrodes across the nanogap, respectively, implying that a 5−10 nm resolution of the probe immobilization technique is needed. Existing probe immobilization techniques are unable to meet this stringent requirement. Fortunately, such a task was successfully accomplished by an electrochemical stripping technique developed in our lab during the course of this work.[26] To provide direct evidence, we chose one representative 5 × 5 cluster and incubated it in a mixture of 1.0 μM FAM (green dye)-labeled oligonucleotides with their base sequences complementary to CPs, and Cy3 (red dye)-labeled oligonucleotides with their base sequence complementary to AP. Figure 1B−D provides a compelling visual proof that we were successful in selectively immobilizing the oligonucleotide probes on the surfaces of all the nanometer-spaced electrodes by using the following procedure: After a thorough cleaning in Nanostrip,[27] AP monolayers were first introduced to both the bottom and the top electrodes. Referring to the fluorescence image in Figure 1B, it is apparent that AP indeed formed excellent monolayers on the surfaces of both electrodes. Now all bottom five electrodes were subjected to electrochemical stripping and a subsequent 2 h incubation period in 1.0 μM CP solution. As shown in Figure 1C, AP was only present on the top electrodes after electrochemical stripping judging from the complete disappearance of the fluorescence at the bottom electrodes. Since a monolayer of AP was already present on the top electrodes, the latter treatment with CP solution would presumably result in the formation of a monolayer of CP on the bottom electrodes. This was corroborated by incubating the 5 × 5 cluster in the mixture of the green and red dye-labeled oligonucleotide solution (Figure 1D). The fluorescence image strongly suggests a high surface coverage of the immobilized probes and excellent hybridization efficiency. Moreover, nonspecific adsorption on the substrate or on the electrode surface was negligible as is evident from the clean and well-confined fluorescence image with a signal/noise ratio of >90/1.

Figure 1E−H shows step-by-step the working principle of the sensor array. Monolayers of CPs and APs are self-assembled on the bottom and top gold electrode across the nanogap, respectively, acting as the bioaffinitive sensing interface (Figure 1E). The interaction of the CP with sample mRNAs forms duplexes, bringing target mRNAs onto the bottom electrode (Figure 1F). The poly(A) tails of the hybridized mRNAs serve anchoring sites, providing the requisite local environment to facilitate bridging across the nanogaps. As a result, the hybridized mRNA strands in the close proximity of the nanogaps are held vertically across the nanogaps after hybridizing with APs on the top electrodes (Figure 1G). And the formation of the hybridized mRNA-templated silver nanowires across the nanogaps provides a much needed sensitivity for the detection of mRNAs (Figure 1H). To minimize nonhybridization-related uptake of mRNAs and to increase the hybridization efficiency, the CPs and APs are designed in a way that there is at least 20 °C difference in melting temperatures. So there is very little hybridization of the poly(A) tails during the target mRNA capturing process (first hybridization). The high density of the anionic AP on the top electrodes alleviates the nonspecific adsorption of mRNA, producing a high signal/noise ratio.

Feasibility Study. In the first feasibility test, 100 ng of total RNA was tested at a sensor array where CP was designed for glyceraldehyde 3-phosphate dehydrogenase (GAPDH) mRNA. Upon hybridizing at 50 °C and annealing at 25 °C for 30 min, respectively, GAPDH was selectively bound to its complementary CP and AP and became fixed on the sensor surface across the nanogap. Silver nanowires were produced alongside the hybridized GAPDH strands via the mRNA-templated silver metallization formation.[28] A typical $i-V$ curve of the sensor after silver treatment

(29) Gonzalez-Pastor, J. E.; Millan, J. L. S.; Moreno, F. *Nature* **1994**, *369*, 281–281.

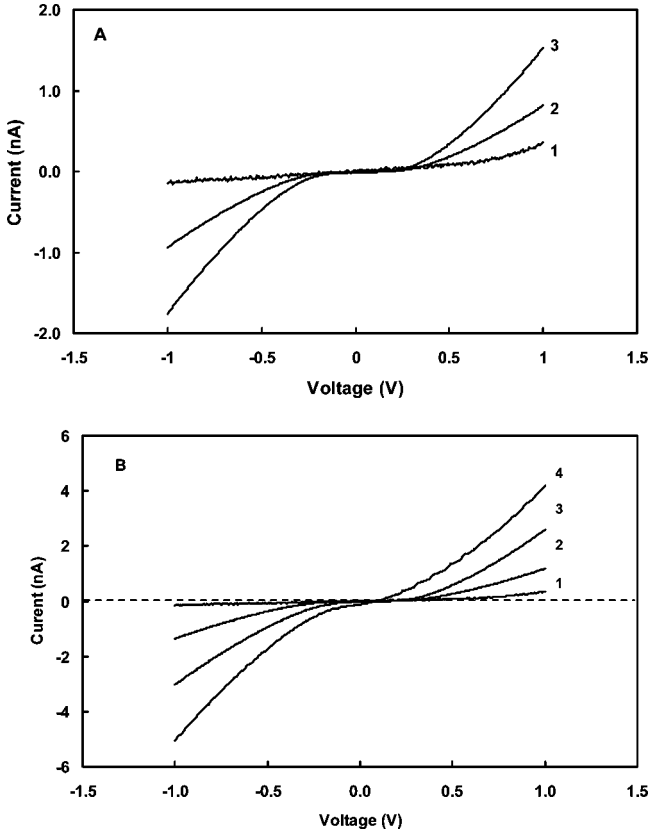

Figure 2. (A) $i-V$ curves of (1) a control, (2) a nanogap sensor with only CP, and (3) a nanogap sensor with both CP and AP in 100 ng of total RNA. For clarity, the $i-V$ curves of the control and the CP-coated sensor were scaled up 200 and 10 times, respectively. (B) $i-V$ curves of (1) 10 ng of total RNA and (2−4) GAPDH spikes in 5.0 fM increments.

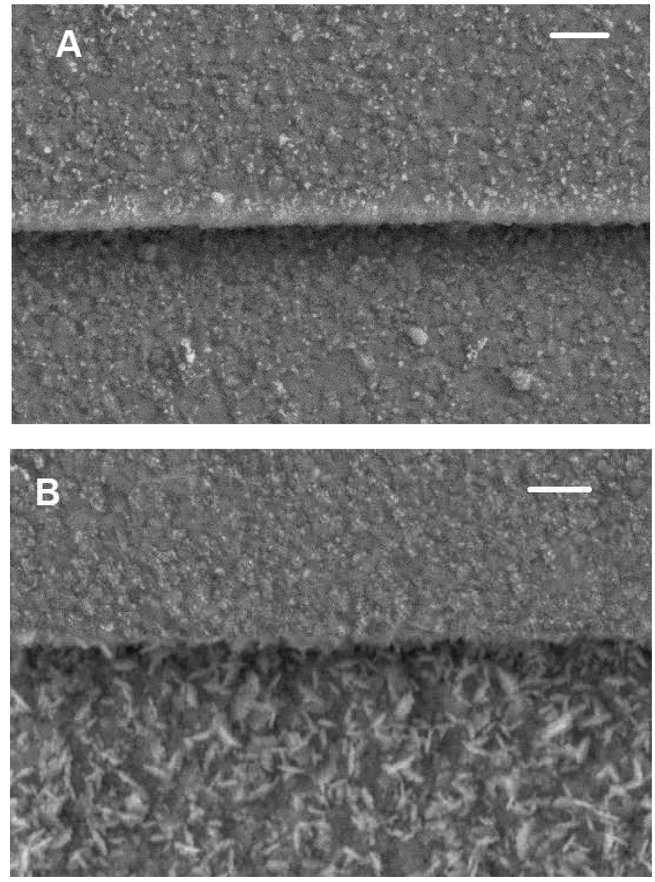

Figure 3. SEM images of 1.0 pM GAPDH-hybridized (A) control sensor and (B) a GAPDH sensor after silver treatment. Scale bar is 25 nm.

is shown in Figure 2A. For comparison, a $i-V$ curve of a sensor in which the bottom electrode was immobilized with noncomplementary CP (control sensor) after the same treatments are also given in Figure 2A. As seen in Figure 2A, a significantly higher current (conductance at 1.0 V, as $S = 1/R = I/U$) was observed at the hybridized sensor than that of the control. Extensive washing and voltage ramping between −1.0 and 1.0 V produced no noticeable changes, revealing that the silver nanowires are robustly bound to the hybridized mRNA stands between the two gold electrodes, effectively bridging the nanogap. It is expected that the hybridizations of the target mRNA to CP and AP resulted in the formation of vertically aligned mRNA strands across the nanogap. When the hybridized sensor array is incubated in the silver metallization solution, silver ions are concentrated and aligned around the hybridized mRNA strands through electrostatic interaction and chemical bonding.[30] This high silver concentration around the mRNA provides a local environment of high density of silver nucleation centers after reduction that facilitates a predominant formation of silver nanowires alongside the mRNA strands, offering the much desired architecture for high conductance. The sizable increase in conductance clearly indicated that an electron-conducting path is formed across the nanogap as a result of hybridization and silver metallization. The extremely low conductance of the control implies that the nonhybridization-related signal of this array is negligible, which facilitates the detection of mRNA at ultralow concentrations. In addition, the $i-V$ was nonlinear, which is likely to be caused by intergrain boundary resistance in the silver nanowires.[31]

To verify whether the two-probe approach is beneficial in the detection of mRNA, a sensor array coated with only monolayers of CP for GAPDH at both top and bottom electrodes was also tested in the total RNA solution. As shown in Figure 2A, the conductance was ~50-fold higher than that of the control, but only $\sim 1/20$ of that obtained with the two-probe sensor array. Since the length of GAPDH is significantly longer than the nanogap, some of the hybridized GAPDH strands are able to cross the nanogap naturally. Subsequent silver metallization produces some silver nanowires across the nanogap.

To further verify that the conductance change is indeed due to the hybridized GAPDH, successive aliquots of GAPDH cDNA were spiked into the total RNA in 5.0 fM increments before hybridization. As shown in Figure 2B, further increases in conductance were observed. The signals observed for the spiked-in total RNA increased almost linearly with the increase in GAPDH cDNA concentration, suggesting that the signal generated in the total RNA sample is originated from GAPDH mRNA and giving a preliminary indication of the reproducibility of the sensor array.

Figure 3 shows SEM images of the control and the GAPDH-hybridized sensor. As seen in Figure 3A, there was some silver deposition at the control sensor since the two gold electrodes are

(30) Hossain, Z.; Huq, F. *J. Inorg. Biochem.* **2002**, *91*, 398–404.

(31) Heinzel, T. *Mesoscopic Electronics in Solid State Nanostructures*; Wiley-VCH: Weinheim, Germany, 2003; p 225.

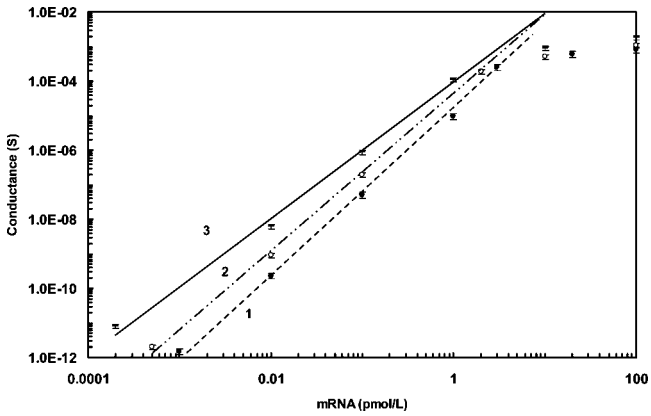

Figure 4. Calibration curves for (1) BRCA1, (2) GAPDH, and (3) His4.

covered with monolayers of CP and AP, respectively, and the silver formation is largely on any nucleic acid molecule. However, due to the vertical arrangement of the nanogap, even the formation of a thin silver film at the two gold electrodes, particularly the bottom electrode, does not generate a measurable signal as long as the silver film is not thick enough to bridge the nanogap. However, there was a distinct difference between the control and the GAPDH-hybridized sensor. Only the hybridized sensor showed silver nanowire formation at the bottom electrode (Figure 3B). And more importantly, there were indeed some silver nanowires aligned across the vertical nanogap, which are responsible for establishing the electron-conducting path across the nanogap.

Calibration Curve. The applicability of the proposed sensor array in mRNA expression profiling was then tested on genomic samples. In this study, three full-length genes (cDNA), namely, histone H4 (His4, 312 bp), GAPDH (1008 bp), and breast cancer gene 1 (BRCA1, 5592 bp), covering both high/low copy number and long/short genes, were used as calibration standards. For the control experiments, noncomplementary CPs were used in the sensor array preparation. As illustrated in Figure 4, the dynamic ranges for His4, GAPDH, and BRCA1 were 0.2 fM to 100 pM, 0.5 fM to 50 pM, and 1.0 fM to 50 pM, with relative standard deviations of <10% and detection limits of 0.10, 0.20, and 0.30 fM, respectively. In comparison to the best direct mRNA detection procedures, the sensitivity was improved by at least an order of magnitude.[21−23] In the proposed sensor array, the hybridized mRNA strands are forced to line up across the nanogap, which greatly enhances the bridging power and hence the sensitivity and detection limit. The sensitivity now is determined by the density and diameter of the silver nanowires, which in turn are determined by the total number of aligned mRNA strands across the nanogap and silver metallization. Hypothetically, if silver metallization and hybridization efficiency remain unchanged for all mRNAs, the same signal intensity (conductance per unit concentration) and detection limit should be obtained. However, it was found that both the sensitivity and the detection limit are dependent on the length of the target mRNA—the longer the mRNA, the higher the signal intensity and the detection limit, with no straightforward relationship between the length and the signal intensity (or detection limit) observed, suggesting that the metallization and hybridization efficiency are also dependent on the length of the target mRNA. It is understandable that lower hybridization efficiency is expected with longer target mRNA and hence the higher detection limit. The slightly higher signal sensitivity (slope of the calibration curve) could be a result of the formation of broader silver nanowires alongside the longer mRNAs due to the existence of secondary structures in the unhybridized regions.[32,33]

As shown in Figure 4, at the high-concentration end of the calibration curve, the conductance reached as high as millisiemens, 9 orders of magnitude higher than the background, which translates into a relative change of $\sim 2 \times 10^4$% per unit concentration, far better than any other electrical transduction-based biosensors.[24,25,34] This huge signal intensity is mainly due to a significantly reduced background conductance (<1.0 pS) achieved with the vertical nanogap since planar nano- and microgap devices can also produce a conductance at millisiemen levels, but on a huge background of submicrosiemens.[24,25,34] Unlike the planar nano- and microstructures where all target DNA strands, hybridized, loosely bound, and nonspecifically adsorbed, contribute to the conductance of the device,[24,25,34] the extremely low background suggests that the unique vertical arrangement and the two-step hybridization approach significantly reduce the background to a level comparable to the instrument noise, since bridging is attained only when both the 5′-end and 3′-end of the target mRNA strand hybridize with the CP and AP, respectively. In other words, to generate a conductance increment the target mRNA strand must be "held" vertically by the CP and AP across the nanogap. Messenger RNA strands found lying at the bottom electrode have very little effect on the conductance.

Specificity Study. To evaluate the capability of the sensor array in discriminating mismatches, three CPs for GAPDH, namely, complementary, one-base-mismatched (OBM), and two-base-mismatched (TBM), were immobilized on the bottom electrodes, respectively. The corresponding array was employed in the detection of 10 fM and 1.0 pM GAPDH. It was found that the sensor array offers excellent discrimination against mismatched sequences. As seen in Figure 5, irrespective to the concentration, the normalized conductance (100% for the full complementary CP) dropped by ∼95% when the OBM CP was used and by ∼99% when the TBM CP was used, which translate into a single-base mismatch selectivity of ∼20/1 and two-base mismatch selectivity of ∼99/1, respectively, far better than most optical and micro- and nanogap-based electrical nucleic acid biosensors.[24,25,34−36] Moreover, the conductance was indistinguishable from the background level when three bases were mismatched in the CP. The good mismatch discrimination is probably also originated from the unique vertical arrangement of the nanogap and the two-step hybridization procedure.

Application. With the much improved sensitivity, the sensor array allowed us to direct profile mRNA expression in real-world samples—total RNAs extracted from breast cancer tissues, normal breast tissues, and MCF-7 cells. Expression levels of the three representative mRNAs were determined by the sensor array and

(32) Hofacker, I. L.; Fekete, M.; Stadler, P. F. *J. Mol. Biol.* **2002**, *319*, 1059–1066.
(33) Eddy, S. *Nat. Rev. Genet.* **2001**, *2*, 919–929.
(34) Fan, Y.; Chen, X.; Trigg, A. D.; Tung, C.; Kong, J.; Gao, Z. *J. Am. Chem. Soc.* **2007**, *129*, 5437–5443.
(35) Fan, Y.; Chen, X.; Kong, J.; Tong, C.; Gao, Z. *Angew. Chem., Int. Ed.* **2007**, *46*, 2051–2054.
(36) Gao, Z. Q.; Yang, Z. Q. *Anal. Chem.* **2006**, *78*, 1470–1477.

Table 2. Analysis of mRNAs in Total RNA

	GAPDH (copy/μg of RNA)	His4 (copy/μg of RNA)	BCRA1 (copy/μg of RNA)
normal breast tissue	$9.3 \pm 0.68 \times 10^6$	$1.4 \pm 0.13 \times 10^6$	$0.28 \pm 0.024 \times 10^6$
	$(9.6 \pm 0.60 \times 10^6)$[a]	$(1.2 \pm 0.31 \times 10^6)$	$(0.23 \pm 0.022 \times 10^6)$
breast cancer tissue	$10.6 \pm 0.72 \times 10^6$	$1.8 \pm 0.14 \times 10^6$	$0.58 \pm 0.036 \times 10^6$
	$(10.8 \pm 0.73 \times 10^6)$	$(1.9 \pm 0.21 \times 10^6)$	$(0.53 \pm 0.032 \times 10^6)$
MCF-7 cells	$13.2 \pm 0.88 \times 10^6$	$3.4 \pm 0.33 \times 10^6$	$0.48 \pm 0.032 \times 10^6$
	$(13.6 \pm 0.90 \times 10^6)$	$(3.6 \pm 0.31 \times 10^6)$	$(0.46 \pm 0.035 \times 10^6)$

[a] Data in brackets were obtained with RT-qPCR.

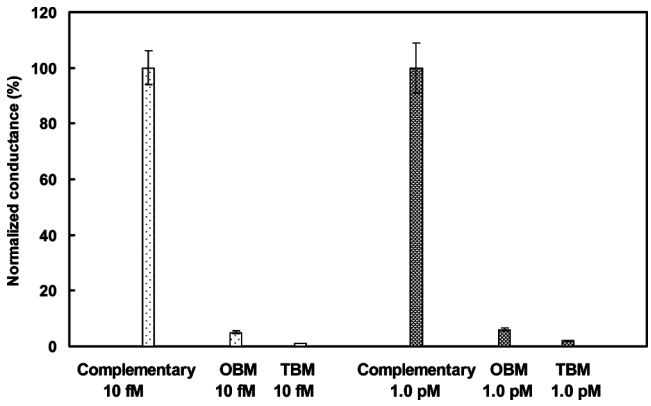

Figure 5. Normalized conductance values of sensor arrays hybridized with complementary and mismatched target mRNAs at 10 fM and 1.0 pM, respectively.

by RT-qPCR and normalized to total RNA. As listed in Table 2, the results obtained with the array were in good agreement with those of RT-qPCR on the same sample. The relative errors associated with the mRNA expression profiling on individual mRNAs were generally less than 10% in the concentration range of 2.5 fM to 1.0 pM. Therefore, it allows us to identify mRNAs with less than 50% difference ($>3 \times 10\%$) in expression levels under two conditions, a substantial improvement over existing gene expression techniques.[7,37] It is advantageous because the expressions of many of the most interesting mRNAs often differ slightly under different conditions. As compared to the conventional mRNA expression techniques, with the greatly improved sensitivity the proposed sensor array offers a greater accuracy in the identification of differentially expressed mRNAs and significantly reduces the amount of total RNA needed from micrograms to nanograms.

The electrical sensor array described above is largely immune to sample-dependent bias as it measures mRNA directly and simultaneously. An assay that directly utilizes total RNA minimizes the inevitable sample losses in more complex protocols requiring RNA size fractionation or multiple purification steps. A quantitative assay requires that each step proceed in a reproducibly high yield and be insensitive to small deviations from the standard protocol. These goals are facilitated if there are no amplifications or minimal separation steps that can introduce sample-dependent variations and if both tagging and hybridization reach steady state near equilibrium, minimally dependent on reaction kinetics or concentrations. The proposed sensor array allows hybridization to proceed simultaneously and far toward equilibrium under practically identical conditions. And the similar melting temperatures of the CPs ensure that most mRNAs will be predominately hybridized at equilibrium.

CONCLUSION

In summary, we have developed a simple, rapid, and sensitive PCR-free electrical sensor array for mRNA expression profiling. The potential of the electrical sensor array for PCR-free mRNA expression profiling was demonstrated with total RNAs extracted from various samples. The sensor array also offers the possibility of parallel analysis of up to 80 mRNAs on a single chip, making it suitable for application in clinical diagnostics and drug discovery. The advantages of the sensor array developed in this work, such as the ultrahigh signal-to-noise ratio and minimal sample preparation, enhance the suitability of this array for the adaptation to miniaturized analytical platforms. This electrical sensor array is promising to be an attractive alternative for gene expression profiling and may enable the development of a simple, low-cost, and portable multiplexing mRNA profiling system, opening the door to molecular diagnostics, particularly for early cancer diagnosis, point-of-care, and field uses.

Received for review February 4, 2010. Accepted June 12, 2010.

AC1003135

(37) Brazeau, D. A. *Drug Discovery Today* **2004**, *9*, 838–845.